Cycloaddition Reactions of 1,3-Dimethylallene. Assignment of Stereochemistry of the Cycloadducts and Interpretation of Product Distributions

Daniel J. Pasto,* Kiyoaki D. Sugi, and James L. Malandra

Department of Chemistry and Biochemistry, University of Notre Dame, Notre Dame, Indiana 46556

Received July 26, 1990

The structures of the cycloadducts formed in the (2 + 2) cycloaddition reactions of 1,3-dimethylallene (13DMA) with 1,1-dichloro-2,2-difluoroethene (1122), acrylonitrile (ACN), methyl acrylate (MAC), *N*-phenylmaleimide (NPMI), and diethyl fumarate (DEF) and maleate (DEM) and the product distributions have been interpreted on the basis of favored conformations for diradical formation and ring closure to the cycloadducts. The stereochemistry of the ring substitution in the cycloadducts derived from ACN and MAC has been assigned on the basis of the relative chemical shifts of H_2, the relative magnitudes of the vicinal coupling constants between H_1 and H_2, the relative magnitudes of the cross-ring coupling constants between H_1 and H_3 and H_4, which are highly dependent on the conformations of the substituted methylenecyclobutane ring systems, and, in the case of the ACN cycloadducts, the results of NOE studies. The stereochemistry about the exocyclic double bonds in the cycloadducts derived from 13DMA with 1122, ACN, and MAC has been assigned on the basis of the relative magnitudes of the allylic and homoallylic coupling constants between H_1, H_3, and H_4 with H_5 and CH_{3b}, the interpretation of which is based on the results of conformational studies carried out by molecular mechanics and ab initio MO calculations on methylenecyclobutane (**28**), pseudoaxial and pseudoequatorial 2-methylmethylenecyclobutane (**29a** and **29e**), ethylidenecyclobutane (**30**), and pseudoaxial and pseudoequatorial 2-methylethylidenecyclobutane (**31a** and **31e**). The results of these calculations indicate that with **29** the pseudoaxial conformation **29a** is significantly populated, while with **31** the pseudoaxial conformation **31a** should be overwhelmingly populated. The trends in the relative chemical shifts and the magnitudes of the vicinal and long-range coupling constants observed in the NMR spectra of the cycloadducts derived from the reaction of 13DMA with NPMI and DEF have allowed for the assignment of the stereochemistry about the exocyclic double bonds and the ring substitution of the cycloadducts formed in these reactions. The product distributions formed in the cycloaddition reactions of 13DMA with ACN and NPMI have been analyzed by molecular mechanics calculations on the conformational preferences for formation of the diradical intermediates and on the conformational preferences of the diradical intermediates which lead directly to cycloadduct formation. The predictions of the molecular mechanics calculations are in agreement with the observed configurations in the cycloadducts formed from (*R*)-(−)-13DMA and ACN and consistent with the observed product distributions. Detailed analyses of the observed product distributions in the cycloaddition reactions of 13DMA with the various radicophiles lead to the conclusions that in the cycloaddition reaction with 1122 the anti,anti diradical intermediate is preferentially formed, while in the cycloadditions reactions with ACN, MAC, and NPMI the anti,syn diradical intermediates are preferentially formed. The differences in stereochemical preferences are discussed in terms of possible differences in the degree of development of the transition states for diradical intermediate formation with different dominant steric interactions. The cycloaddition with DEM produces only trans diester products and also results in the isomerization of DEM to DEF. These data imply the reversible formation of the diradical intermediates from DEF and DEM, as well as internal rotation occurring competitive with ring closure.

Introduction

Recent studies in our laboratories have focused on the factors controlling the stereoselectivity in the formation of the diradical intermediates formed in (2 + 2) cycloaddition reactions of alkyl-substituted allenes and the competition between ring closure, internal rotation, and cleavage of the intermediate diradicals.[1-3] In the cycloaddition reactions of monoalkyl-substituted allenes with various radicophiles (represented as C=C in the equation), the diradical intermediate having the stereochemistry about the allyl radical portion of the intermediate shown in **1** is formed in preference to that shown in **2** as implied by the predominant formation of **3** over **4**. **5** is a minor product that can be formed from both **1** and **2**. The preference for the formation of **1** increases with increasing size of the alkyl group R, with **1** apparently being the only intermediate formed in the cycloaddition reaction of *tert*-butylallene with 1,1-dichloro-2,2-difluoroethene (1122);[3] the cycloaddition reaction of 1122 with alkyl-substituted allenes being used as a model for a two-step diradical intermediate cycloaddition process.[3] This preference for the formation of **1** has been attributed to the

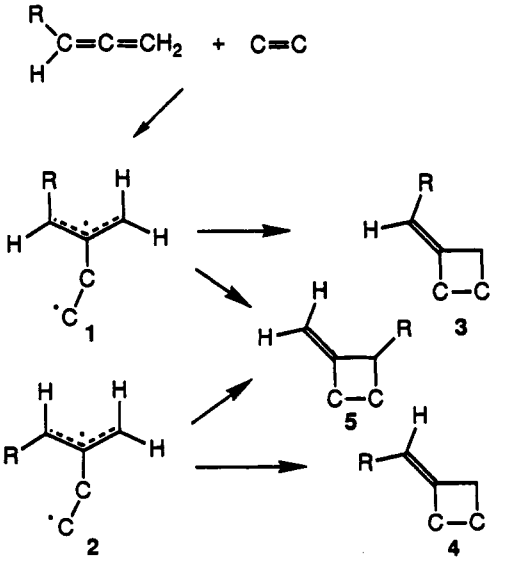

greater steric congestion encountered when the R group at the terminus of the allene rotates toward the approaching radicophile, as shown in the transition state represented as **7**, compared to when the R group rotates away from the approaching radicophile as shown in the transition state represented as **6**. Evidence that attack on

(1) Pasto, D. J.; Yang, S.-H. *J. Am. Chem. Soc.* **1984**, *106*, 152.
(2) Pasto, D. J.; Heid, P. F.; Warren, S. E. *J. Am. Chem. Soc.* **1982**, *104*, 3676.
(3) Pasto, D. J.; Warren, S. E. *J. Am. Chem. Soc.* **1982**, *104*, 3670.

0022-3263/91/1956-3781$02.50/0

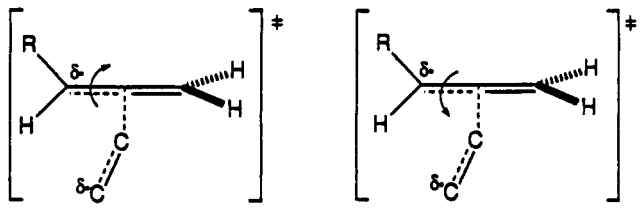

6 7

C_2 of the more highly substituted C_1–C_2 double bond occurs in the cycloaddition reactions with 1122 and other dienophiles has been derived from the results of extensive kinetic isotope effect studies.[1-4]

Product distributions derived from the cycloaddition reactions of *tert*-butyl-[1] and phenylallene[5] with sevral radicophiles suggest that in certain cases the formation of the diradical intermediate is reversible as evidenced by the predominant formation of cycloadducts having the stereochemistry shown in **4**. This reversibility has been attributed to increased steric strain in the allyl radical portion of intermediate **1** when the large R group is in the anti position. This steric strain raises the ground-state energy of the intermediate relative to that of the transition state for cleavage, allowing for cleavage of the intermediate to be competitive with ring closure.

The observation that increased steric strain in the allyl radical portion of the diradical intermediates might induce reversible formation of the diradical intermediates suggested that the anti,anti diradical intermediates formed in the cycloaddition reactions of 1,3-dialkyl-substituted allenes should also suffer from such steric strain and might be formed in reversible processes. This has led us to investigate the cycloaddition reactions of 1,3-dimethylallene (13DMA) with various radicophiles. The predominant formation of products having the stereochemistry about the exocyclic double bond as shown in **4** would be suggestive of, but not conclusive for, the reversible formation of the diradical intermediates. The reversible formation of the diradical intermediates in cases where there is no possibility of observing stereospecificity in diradical and product formation might be detected by the use of an optically active 1,3-dialkyl-substituted allene.

The cycloaddition of optically active 13DMA with acrylonitrile (ACN) has been studied by Baldwin and Roy.[6] The cycloaddition of (*R*)-13DMA with ACN produced four cycloadducts, all of which were optically active and assigned the *R* configuration at C_2 of the cyclobutane ring after ozonolysis to the corresponding cyclobutanones and analysis by ORD.[6,7] The formation of four optically active cycloadducts led the authors to postulate the formation of the chiral diradical intermediates represented as **8** and **9** that are formed by the least sterically hindered approach of the ACN to the 13DMA resulting in one methyl group ultimately being in the anti position with the methyl group at the other terminus of the 13DMA rotating toward the approaching radicophile resulting in the formation of **8** and **9**.[6] However, the results obtained in the authors' laboratories on the cycloaddition reactions with monoalkyl-substituted allenes with 1122 would lead one to predict the predominant formation of the diradical intermediate **10** in which the radicophile approaches the least sterically

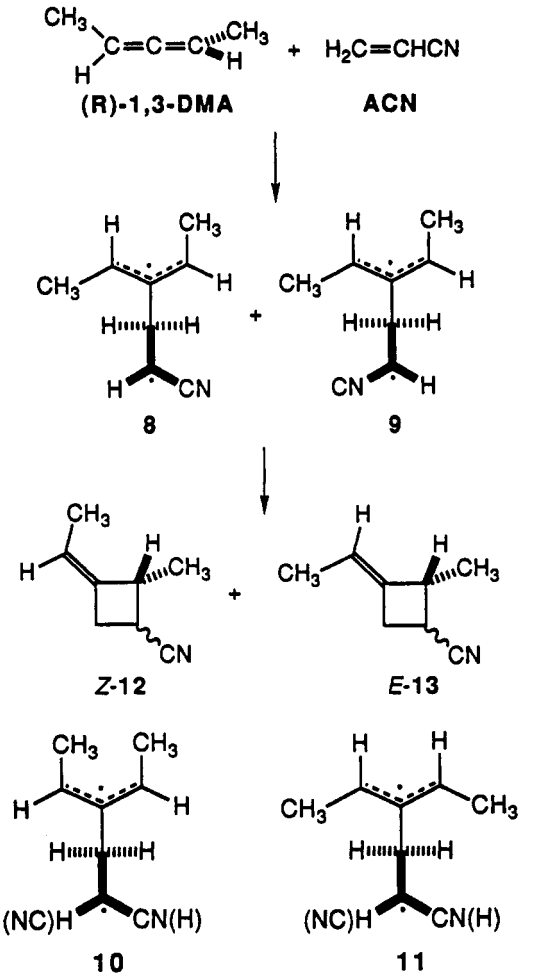

hindered face of one of the double bonds of the 13DMA with the methyl group at the other end of the 13DMA preferentially rotating away from the approaching dienophile. Diradical intermediate **11** is not expected to be formed to any significant extent, its formation involving the more sterically congested approach of the reactants and the less favored direction of rotation of the terminus of the 13DMA. As such, syn,syn diradical intermediates such as **11** will not be considered as viable intermediates in the discussions of the cycloaddition reactions of 13DMA with various radicophiles in this article. Ring closure of the diradical intermediates **8** and **9** result in the formation of the cis- and trans-*E* and -*Z* cycloadducts **12** and **13**. The ring closure of **10**, however, results in the formation of only the cis and trans isomers of **12**. Unfortunately, neither the product distribution or the stereochemistry of the four stereoisomeric cycloadducts derived from the cycloaddition of 13DMA with ACN was reported; however, as will be evidenced later, it was probably not possible to unambiguously assign the stereochemistry of the cycloadducts by the techniques available to the authors at that time.

As a prelude to a detailed stereochemical investigation of the cycloaddition reactions of optically active 1,3-disubstituted allenes with various radicophiles, we have carried out a stereochemical study of the cycloaddition reactions of racemic 13DMA with 1122, ACN, methyl acrylate (MAC), *N*-phenylmaleimide (NPMI), diethyl fumarate (DEF), and diethyl maleate (DEM). The results of these studies collectively provide detailed information on the steric interactions involved in the formation of the diradical intermediates, the preferred conformations of the intermediates, and the factors that determine their mode of ring closure.

(4) Pasto, D. J.; Warren, S. E.; Weyenberg, T. *J. Org. Chem.* **1986**, *51*, 2106. Pasto, D. J.; Huang, N.-Z. *Ibid.* **1986**, *51*, 412.
(5) Pasto, D. J.; Yang, S.-H. *J. Org. Chem.* **1986**, *51*, 1676.
(6) Baldwin, J. E.; Roy, U. V. *J. Chem. Soc. D* **1969**, 1225.
(7) In this article, the cycloaddition reactions of 13DMA will be illustrated using (*R*)-1,3-DMA with formation of the *R* configuration at C_2 of the cycloadducts for clarity and uniformity in discussing the overall stereochemistry of the cycloaddition reactions.

Table I. ^{1}H Chemical Shifts and Coupling Constants in 16 and 17

16		17	
δ	J (Hz)	δ	J (Hz)
CH_{3a}, 1.38	CH_{3a}-H_1, 7.07	CH_{3a}, 1.28	CH_{3a}-H_1, 7.07
CH_{3b}, 1.76	CH_{3b}-H_2, 7.10	CH_{3b}, 1.86	CH_{3b}-H_2, 7.15
H_1, 3.43	CH_{3b}-H_1, 2.18	H_1, 3.31	CH_{3b}-H_1, 2.96
H_2, 6.19	CH_{3b}-F, 3.40	H_2, 5.75	CH_{3b}-F_1, 3.12
	H_1-H_2, 2.97		CH_{3b}-F2, 2.28
	H_2-F, 2.99		H_1-H_2, 2.67
	CH_{3a}-F, 0.8		CH_{3a}-F, 0.76
			H_2-F_1, 0.99
			H_2-F_2, 0.42

Results and Discussion

Cycloaddition of 13DMA with 1,1-Dichloro-2,2-difluoroethene. The reaction of 13DMA with 1122 quantitatively produces a mixture of two cycloadducts in a 66.6:33.4 ratio that have been assigned structures **16** and **17**. The stereochemistry about the exocyclic double bonds

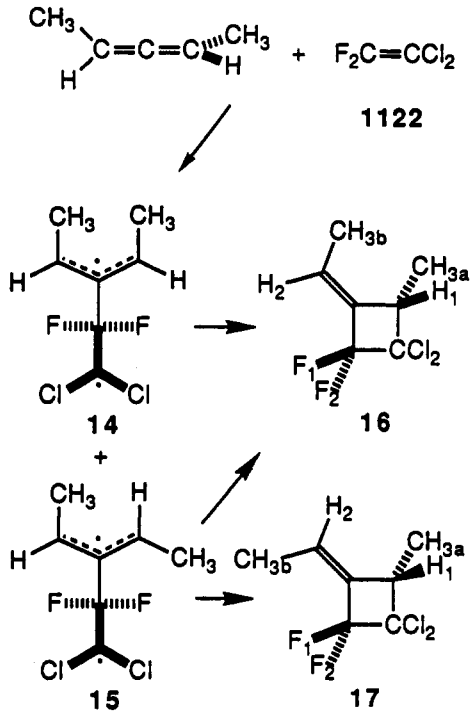

in **16** and **17** has been assigned on the basis of the relative chemical shifts of the vinyl hydrogen and methyl groups and the relative magnitudes of the long-range allylic and homoallylic H–H and H–F coupling constants which have been identified by extensive double resonance studies on the two cycloadducts (Table I). In cycloadducts of 1122, the vinyl hydrogens appear ~0.4 ppm to lower field when syn to the CF_2 group, while the allylic hydrogens appear ~0.1–0.2 ppm to lower field when syn to the CF_2 group.[1] And, in general, cis allylic long-range coupling constants are larger than trans allylic coupling constants,[8] while trans homoallylic coupling constants are generally larger than cis homoallylic coupling constants,[8] although the relative magnitudes of these long-range coupling constants are quite sensitive to the dihedral angle between the C–H bond and the intervening π bond, being maximum when the C–H bond is coaxially aligned with the p AO's of the π system.[8]

The vinyl hydrogen in the major isomer appears at δ 6.19 compared to δ 5.75 in the minor isomer, while the vinyl methyl group appears at δ 1.76 in the major isomer compared to δ 1.86 in the minor isomer. These data suggest that the major isomer possesses the stereochemistry about the exocyclic double bond shown in structure **16** and the minor isomer that shown in structure **17**. These stereochemical assignments are supported to a major extent by the relative magnitudes of the allylic and homoallylic H–H and H–F coupling constants. The long-range, homoallylic coupling constant between H_1 and CH_{3b} in **16** (2.18 Hz) is less than that observed in **17** (2.96 Hz), while the homoallylic coupling constant between the two fluorine atoms and H_2 in **16** is greater (3.40 Hz) than that observed in **17** (2.28 and 3.12 Hz). The long-range, allylic coupling constant between the two fluorine atoms in **16** (2.99 Hz) is greater than that in **17** (<0.3 Hz), which is consistent with the assigned stereochemistry. The long-range, allylic coupling constants between H_1 and H_2 are not, however, consistent with the stereochemical assignments, being greater in **16** (2.97 Hz) than in **17** (2.67 Hz). Overall, however, the majority of the NMR evidence is consistent with the stereochemical assignments shown in structures **16** and **17** for the major and minor isomers.

There are some very interesting differences in the NMR spectra of **16** and **17** that merit noting. The vinyl methyl group in **16** appears as a ddt[9] with coupling constants of 7.10 ($J_{H_2CH_{3b}}$), 2.18 ($J_{H_1-CH_{3b}}$), and 3.40 Hz (t, $J_{F-CH_{3b}}$). The vinyl hydrogen appears as a dtq with coupling constants of ~2.9 ($J_{H_1-H_2}$), 2.99 (t, J_{F-H_2}), and 7.10 Hz. In both cases, the two diastereotopic fluorine atoms (δ 54.0 and 56.4 relative to external BF_3-etherate with J_{FF} 200 Hz) interact with H_2 and CH_{3b} with the same value of J. In **17**, such is not the case. The vinyl methyl resonance of **17** appears as a dddd with coupling constants of 3.12 ($J_{F_1-CH_{3b}}$), 2.96 ($J_{H_1-CH_{3b}}$), 2.28 ($J_{F_2-CH_{3b}}$), and 7.15 Hz. In this case, the two diastereotopic fluorine atoms (δ 52.3 and 54.7 with J_{FF} 197 Hz) are coupled with the vinyl methyl group with different coupling constants. The long-range coupling between F_1 and F_2 with H_2 is not observable and must be less than 0.3 Hz.

Cycloadduct **17** can be formed only from the diradical intermediate **15** by ring closure to the left end of the allyl radical in **15**. Ring closure of **15** involving the right end of the allyl radical produces **16**. Of the two modes of ring closure, the transition state for ring closure to the left end of the allyl radical to form **17** should be less sterically congested and thus favor the formation of **17**; however, it is not possible to determine quantitatively the relative extents of the two modes of ring closure of **15**. Ring closure of the diradical intermediate **14** at either end of the allyl radical produces only **16**. As **16** is the major product, one must conclude that **14** is formed to a greater extent than **15**. This is consistent with prior conclusions that the diradical intermediates formed in the cycloaddition reactions with 1122 are formed irreversibly and that the preferred stereochemistry in the diradical intermediates formed in these cycloaddition reactions with substituted allenes is controlled by the steric interactions generated between the approaching radicophile and the alkyl group at the terminus of the rotating end of the allene and not by the steric interactions present in the diradical intermediate despite the fact that the transition states for the formation of the diradical intermediates appears to occur very late along the reaction coordinates. The diradical intermediate **14** is considerably more sterically congested than in the case of the diradical intermediates formed in the cycloaddition reactions of 1122 with monoalkyl-substituted allenes;

(8) Barfield, M.; Sternhall, S. *J. Am. Chem. Soc.* **1972**, *94*, 1907.

(9) The multiplicities will be specified as d for doublet, t for triplet, and q for quartet. For multiple couplings to a given nucleus, the patterns will be referred to as dt for double triplet, etc.

Table II. ^{1}H Chemical Shifts and Coupling Constants in 20–23

	20	21	22	23
	Chemical Shifts (δ)			
CH_{3a}	1.41	1.34	1.31	1.23
CH_{3b}	1.55	1.57	1.51	1.53
H_1	3.34	3.42	3.24	3.33
H_2	3.23	2.57	3.23	2.58
H_3	2.96	2.87	2.94	2.91
H_4	2.99	2.95	3.03	3.01
H_5	5.22	5.23	5.26	5.25
	Coupling Constants (Hz)			
H_1–H_2	8.80	6.89	8.62	7.96
H_2–H_4	8.80	6.89	8.62	7.96
H_2–H_3	7.31	9.50	5.59	9.00
H_1–H_5	2.35	2.46	1.40	2.20
H_3–H_5	1.92	1.77	1.75	2.91
H_4–H_5	1.92	1.77	1.75	2.32
H_1–H_3		~0.6		1.16
H_1–H_4		2.74		2.53
H_1–CH_{3a}	7.06	7.07	7.06	7.06
H_1–CH_{3b}	2.24	2.01	1.19	1.94
H_3–CH_{3b}	2.02	2.01	1.37	2.37
H_4–CH_{3b}	2.02	2.01	1.37	1.35
H_5–CH_{3b}	6.82	6.96	6.81	6.77

however, 14 appears to be formed irreversibly.[3]

Cycloaddition of 13DMA with Acrylonitrile. The cycloaddition of 13DMA with ACN quantitatively produces a mixture of the four cycloadducts **20–23** (the relative yields are shown in parentheses), which were isolated by preparative GLC.

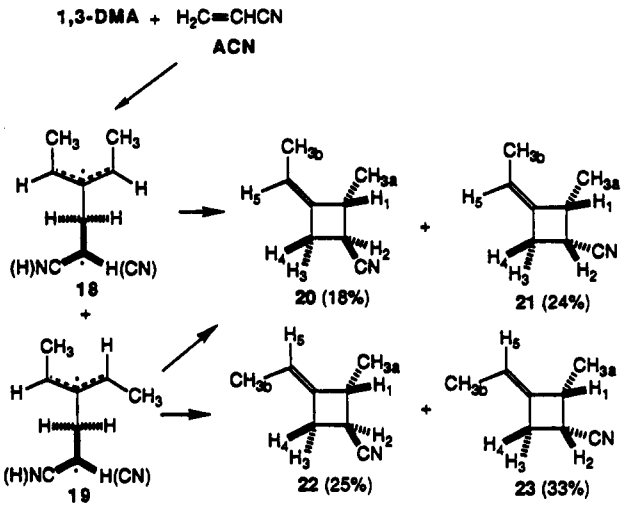

The assignment of the stereochemistry of the ring substitution was not obvious from the relative magnitudes of the vicinal and long-range, cross-ring coupling constants and the relative chemical shifts of the ring protons. In general, when similar substitution patterns exist, cross-ring pseudoequatorial–pseudoequatorial (ee) coupling constants are larger (3–5 Hz) than pseudoaxial–pseudoequatorial (ae) coupling constants (~1 Hz), which are in turn much larger than pseudoaxial–pseudoaxial (aa) coupling constants.[10] There was, however, no consistent interpretation of the chemical shift and coupling constant data of the four cycloadducts. The ^{1}H NMR chemical shifts and coupling constants, determined by extensive decoupling experiments, appear in Table II.

A quick inspection of the ^{1}H chemical shifts in **20–23** shows that the most characteristic differences are in the chemical shifts of H_2. In **21** and **23**, H_2 appears at considerably higher field (δ 2.57 and 2.58) than in **20** and **22** (δ 3.23 and 3.23). This suggests that in the predominant conformations of **21** and **23** H_2 is oriented pseudoaxially, while in **20** and **22** H_2 is oriented pseudoequatorially. The larger vicinal coupling constants between H_3 and H_2 in **21** and **23** indicate that H_3 is oriented pseudoaxially, while the smaller coupling constants between H_1 and H_4 with H_2 indicate that H_1 and H_4 are oriented pseudoequatorially as shown in conformations **25b** and **27b** in Scheme I. This requires that the 2-methyl group be oriented pseudoaxially in the predominant conformations of **21** (**25b**) and **23** (**27b**). Although it appeared reasonable that **25b** (X = CN) should be the predominant conformation for **21** because of the presence of "allylic strain"[11] between CH_{3b} and CH_{3a}, it was not obvious that **27b** (X = CN) should also be the predominant conformation of **23**. In order to gain an understanding of the conformational preferences of the substituted methylenecyclobutanes, ab initio and molecular mechanics calculations have been carried out on methylenecyclobutane (**28**),[12] the pseudoaxial and pseudoequatorial conformations of 2-methylmethylenecyclobutane (**29a** and **29e**), ethylidenecyclobutane (**30**), and the

Scheme I

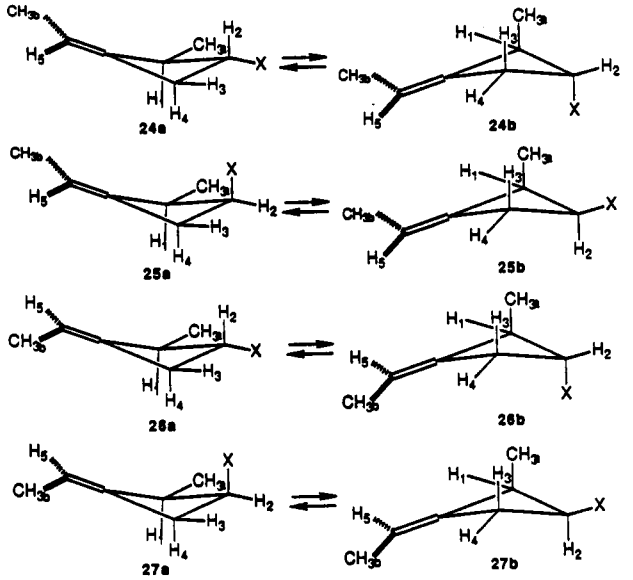

Table III. 3-21G and 6-31G* Total Energies and MM3 Heats of Formation of 28–31

structure	E_{tot} (au) 3-21G	E_{tot} (au) 6-31G*	heat of formation (kcal mol^{-1})
28	−192.86401	−193.94267	29.03
29a	−231.68645	−232.97889[a]	22.36
29e	−231.68624	−232.98001	21.99
30	−231.68610	−232.98097	21.10
31a	−270.50819	−272.01675	14.36
31e	−270.50642[a]	−272.01627[a]	14.81

[a] Not fully optimized value. Value is taken from a fairly flat region of the energy surface with a reasonable geometry.

(10) Wiberg, K. B.; Barth, D. E. *J. Am. Chem. Soc.* **1969**, *91*, 5128.

(11) For a recent review, see: Hoffmann, R. W. *Chem. Rev.* **1989**, *89*, 1841.

(12) Ab initio calculations on methylenecyclobutane at the 3-21G level with geometry optimization with single-point calculations carried out at higher levels on the 3-21G optimized geometry (Skancke, P. N.; Koga, N.; Morokuma, K. *J. Am. Chem. Soc.* **1989**, *111*, 1559. Eckert-Maksic, M.; Maksic, Z. B.; Shancke, A.; Shancke, P. N. *J. Phys. Chem.* **1987**, *91*, 2786); however, the calculated geometrical parameters were not reported in detail. The results of the present calculations differ slightly in the calculated parameters (particularly the nonplanarity of the ring), and the total energies are also slightly different. The reported 6-31G* total energy for **28** was reported to be −193.942 67 au compared to the present value of −193.942 98 au.

pseudoaxial and pseudoequatorial 2-methyl-(*Z*)-ethylidenecyclobutanes (**31a** and **31e**) using the GAUSSIAN86 and -88[13] and Allinger's MM3[14] programs. The total energies derived from the ab initio calculations and the heats of formation derived from the MM3 calculations are given in Table III. The calculated structural parameters are given in Table IV.

The initial ab initio calculations were carried out on **28**, **29a**, and **29e** at the 3-21G basis set level with full geometry optimization. At the 3-21G basis-set level, the pseudoaxial conformation **29a** is calculated to be lower in energy than

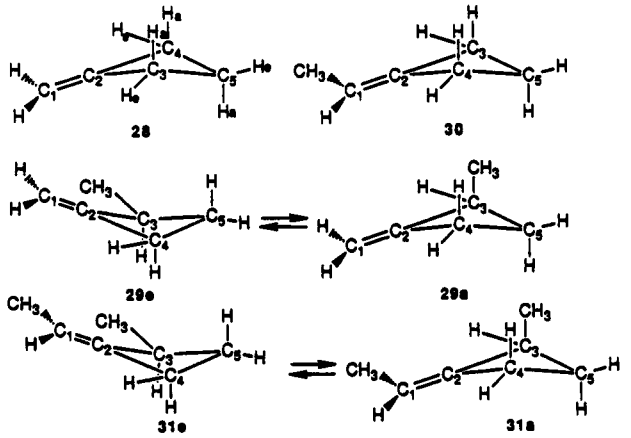

the pseudoequatorial conformation **29e** by 0.13 kcal mol^{-1}. At the 6-31G* level, geometry optimization calculations could not be accomplished on **29a**.[15] The calculations indicated a rather flat energy surface near reasonable structures for **29a**, lying approximately 0.7 kcal mol^{-1} above the geometry-optimized structure of **29e**. MM3 geometry optimization calculations converged on both **29a** and **29e**, with **29e** being indicated to be lower in energy by 0.37 kcal mol^{-1}. There is good correspondence between the 6-31G* and MM3 calculations, which indicates that the pseudoaxial **29a**, although higher in energy, must be substantially populated. Ab initio calculations were also carried out on **31a** and **31e**. Minimum energy structures were found for **31a** at both the 3-21G and 6-31G* levels; however, geometry optimization could not be accomplished on the pseudoequatorial structure **31e**. Again, very flat energy surfaces were encountered. The energies appearing in Table III have been taken from this flat region of the potential energy surface. The results of the calculations on **31a** and **31e** suggest that **31a** is lower in energy by ~1.11 kcal mol^{-1} at the 3-21G level and 0.30 kcal mol^{-1} at the 6-31G* level. MM3 calculations indicate that **31a** is lower in energy by 0.45 kcal mol^{-1}. In the case of **20** and **21**, the results of the calculations indicate that conformations **24b** and **25b** (X = CN) should predominate over conformations **24a** and **25a**. In the case of **22** and **23**, the results of the calculations suggest that conformations **26a** and **27a** (X = CN) should predominate.

The results of the calculations on the conformations of the 2-methyl-1-ethylidenecyclobutane lead to a reasonable interpretation of the NMR spectra of **20**–**23**. The pre-

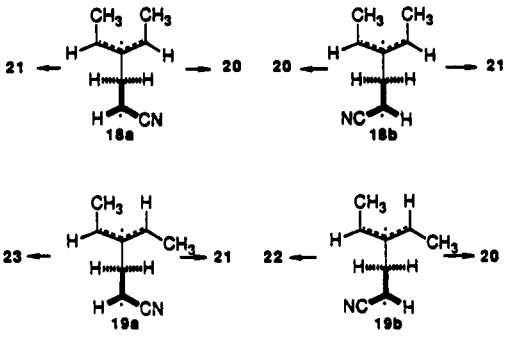

dominant conformations of **21** and **23** are indicated to be **25b** and **27b**, which explains the relative chemical shifts and magnitudes of the cross-ring coupling constants between H_1 and H_3 and H_4. The coupling constants between H_1 and H_4 in **21** and **23** are 2.74 and 2.53 Hz, indicating an ee relationship, whereas the coupling constants between H_1 and H_3 are ~0.6 and 1.16 Hz, indicating an ae relationship. In **21** and **23**, H_3 appears at higher field than H_4, indicating that H_3 is pseudoaxially oriented as shown in **25b** and **27b**. The stereochemistry about the exocyclic double bond in **21** and **23** could not be assigned on the basis of the relative magnitudes of the long-range, allylic and homoallylic coupling constants between H_1 and H_4 (both pseudoequatorial) with H_5 and CH_{3b}. In **21**, the allylic coupling constants suggest an *E* stereochemistry, while no decision can be made on the basis of the homoallylic coupling constants. In **23**, the allylic coupling constants suggest a *Z* stereochemistry, while the homoallylic coupling constants suggest an *E* stereochemistry. The lack of any correlation is probably due to the differences in the environments of H_1 and H_4 and possible slight differences in the dihedral angles involving H_1 and H_4 with the intervening π systems. The stereochemistry about the exocyclic double bonds in **21** and **23** has been inferred from NOE experiments. Irradiation of H_5 in **21** and **23** results in an increase in the intensity of the CH_{3a} resonance by 3.8 and 6.4%, respectively. No change in intensity is observed for H_3 and H_4 resonances in 21 and 23, indicating that **21** possesses the *Z* stereochemistry and **23** the *E* stereochemistry. Preliminary results derived from the cycloaddition of enantioenriched 13DMA with ACN support this assignment of the stereochemistry about the exocyclic double bonds in **21** and **23** (see later discussion).

The lower field chemical shifts of H_2 in **20** and **22** suggest that H_2 is predominantly oriented pseudoequatorially, implying that conformations **24b** and **26b** are populated to a considerable extent. The vicinal coupling constants between H_1, and H_3 and H_4, with H_2, however, suggest that conformations **24a** and **26a** may be dominant. In both **20** and **22** there are two large aa coupling constants and one smaller ae coupling constant. In addition, the pseudoaxial orientation of H_1 results in substantially smaller cross-ring coupling constants between H_1 and H_3 and H_4 that cannot be resolved. It is obvious that the detailed interpretation of the NMR spectral characteristics in terms of conformational populations is quite complicated; however, the general trends support the assigned trans stereochemistry.

The stereochemistry about the exocyclic double bonds in **20** and **22** also cannot be unambiguously assigned on

(13) (a) GAUSSIAN86: Frisch, M. J.; Binkley, J. S.; Schlegel, H. B.; Raghavachari, K.; Melius, C. F.; Martin, L.; Stewart, J. J. P.; Bobrowicz, F. W.; Rohlfing, C. M.; Kahn, L. R.; Defrees, D. J.; Seeger, R.; Whiteside, R. A.; Fox, D. J.; Fleuder, E. M.; Pople, J. A., Carnegie-Mellon Quantum Chemistry Publishing Unit, Pittsburgh, PA, 1984. (b) GAUSSIAN88: Frisch, M. J.; Head-Gordon, M.; Schlegel, H. B.; Raghavachari, K.; Binkley, J. S.; Gonzalez, C.; Defrees, D. J.; Fox, D. J.; Whiteside, R. A.; Seeger, R.; Melius, C. F.; Baker, J.; Martin, R. L.; Kahn, L. R.; Stewart, J. J. P.; Fluder, E. M.; Topiol, S.; Pople, J. A., GAUSSIAN, Inc., Pittsburgh, PA.

(14) MM3: N. L. Allinger, 1989.

(15) It is possible that appropriately close geometries to a potential minimum energy structure for **29e** were not selected as starting geometries, and due to the many interacting structural variables, geometry optimization might not have been able to be achieved.

(16) Not all of the necessary parameters are available in MM3 for the calculations on **29** and **31**. Open-chain parameters were used for those not available in MM3. The torsional parameters used are C_{18}–C_1–C_2–C_3-(C_4) V_1 = –0.300, V_2 = 8.000, V_3 = 0.000; C_{14}–C_3–C_2–C_4 V_1 = 0.060, V_2 = 0.030, V_3 = 1.250; and C_{14}–C_3–C_2–C_1 V_1 = –0.700, V_2 = –0.200, V_3 = –0.550. The bending parameters used are C_{18}–C_1–C_2 KB = 0.470, θ = 122.300; C_{14}–C_3–C_2 KB = 0.540, θ = 109.800.

Table IV. 6-31G* and MM3 Calculated Geometrical Parameters for 28–31[a]

	28		30		29a		29e		31a		31e	
	6-31G*	MM3	6-31G*	MM3	6-31G*	MM3	6-31G*	MM3	6-31G*	MM3	6-31G*	MM3
						Bond						
C_1–C_2	1.314	1.333	1.316	1.335	1.315	1.333	1.315	1.333	1.317	1.335	1.317	1.336
C_1–H_6	1.077	1.102	1.080	1.103	1.077	1.102	1.077	1.102	1.080	1.103		
C_1–H_7	1.077	1.102			1.077	1.102	1.077	1.101			1.080	1.104
C_1–C_{18}			1.504	1.503					1.504	1.503	1.504	1.503
C_{18}–H_{19}			1.084	1.112					1.084	1.112	1.083	1.110
C_{18}–H_{20}			1.087	1.113					1.087	1.113	1.087	1.113
C_{18}–H_{21}			1.087	1.113					1.087	1.113	1.087	1.113
C_2–C_3	1.519	1.525	1.522	1.525	1.524	1.527	1.522	1.527	1.526	1.528	1.529	1.529
C_3–H_8	1.084	1.112	1.085	1.112	1.086	1.114			1.086	1.113		
C_3–H_9	1.086	1.113	1.086	1.113			1.088	1.115			1.087	1.115
C_3–C_{14}					1.527	1.533	1.521	1.530	1.528	1.533	1.526	1.531
C_{14}–H_{15}					1.086	1.113	1.085	1.113	1.086	1.113	1.086	1.113
C_{14}–H_{16}					1.085	1.113	1.086	1.113	1.085	1.113	1.087	1.113
C_{14}–H_{17}					1.087	1.113	1.086	1.113	1.087	1.113	1.085	1.112
C_2–H_4	1.519	1.525	1.520	1.561	1.519	1.524	1.518	1.525	1.519	1.525	1.520	1.526
C_4–H_{10}	1.084	1.112	1.085	1.112	1.084	1.111	1.084	1.111	1.085	1.111	1.085	1.112
C_4–H_{11}	1.086	1.113	1.086	1.113	1.086	1.113	1.086	1.113	1.086	1.113	1.086	1.113
C_3–C_5	1.552	1.561	1.552	1.561	1.556	1.565	1.553	1.562	1.555	1.565	1.526	1.563
C_5–H_{12}	1.083	1.112	1.083	1.112	1.084	1.111	1.084	1.111	1.084	1.111	1.086	1.111
C_5–H_{13}	1.084	1.113	1.084	1.113	1.083	1.113	1.085	1.113	1.084	1.113	1.087	1.113
C_4–C_5	1.552	1.561	1.551	1.561	1.552	1.560	1.550	1.560	1.550	1.560	1.551	1.557
						Bond Angle						
C_2–C_1–H_6	121.6	120.6	118.3	118.8	121.7	120.6	121.6	120.6	118.2	118.8	117.8	118.0
C_2–C_1–H_7	121.6	120.6			121.6	120.6	121.7	120.7				
C_2–C_1–C_{18}			125.4	124.4					125.7	124.5	126.5	126.0
C_1–C_{18}–H_{19}			111.6	112.1					111.8	112.2	112.0	112.5
C_1–C_{18}–H_{20}			111.1	110.9					110.9	110.9	111.3	110.9
C_1–C_{18}–H_{21}			111.0	110.9					111.1	110.9	110.5	110.7
C_1–C_2–C_3	134.0	135.5	134.6	136.0	133.5	135.3	133.9	135.9	134.5	136.0	135.1	137.7
C_2–C_3–H_8	116.8	114.5	116.9	114.6	113.5	112.6			114.4	112.8		
C_2–C_3–H_9	112.5	112.9	113.0	112.9			109.8	111.2			112.0	110.7
C_2–C_3–C_{14}					115.2	113.2	119.2	115.5	115.2	113.3	118.1	117.2
C_3–C_{14}–H_{15}					111.2	112.2	110.9	111.8	111.1	112.2	110.9	111.8
C_3–H_{14}–H_{16}					110.9	111.2	110.8	111.1	111.3	111.3	110.4	111.0
C_3–H_{14}–H_{17}					110.7	111.2	111.1	111.4	110.6	111.2	111.9	111.8
C_1–C_2–C_4	134.0	135.5	133.4	135.1	134.0	135.3	134.0	135.3	133.1	134.8	132.5	133.7
C_2–C_4–H_{10}	116.8	114.5	116.8	114.5	115.9	114.5	117.1	114.7	116.4	114.5	115.7	114.6
C_2–C_4–H_{11}	112.5	112.9	112.9	112.8	113.4	113.1	112.4	113.0	113.4	113.1	113.9	112.9
C_2–C_3–C_5	88.1	90.0	88.2	90.1	88.2	89.3	87.5	89.3	87.8	89.3	88.3	89.5
C_3–C_5–H_{12}	116.6	114.5	116.4	114.5	115.4	114.7	117.0	114.6	115.8	114.7	115.4	114.6
C_3–H_5–H_{13}	112.3	113.0	112.4	113.0	113.4	112.9	111.7	113.1	112.8	112.9	113.2	113.1
C_2–C_4–C_5	88.1	90.0	88.3	90.1	88.5	89.6	87.8	89.4	88.2	90.0	88.7	89.8
						Dihedral Angle						
H_6–C_1–C_2–C_4	3.9	2.1	2.8	2.1	2.1	2.5	4.7	2.8	3.4	2.8	−0.8	0.9
H_7–C_1–C_2–C_3	−3.9	−2.1			−1.6	−2.6	−4.9	−2.9				
C_{18}–C_1–C_2–C_3			−3.5	−2.4					−2.6	−2.9	−2.5	−3.8
H_{19}–C_{18}–C_1–C_2			0.5	−0.6					2.7	0.2	−5.5	−6.6
H_{20}–C_{18}–C_1–C_2			121.1	119.6					123.2	120.4	115.6	114.1
H_{21}–C_{18}–C_1–C_2			−120.0	−120.8					−118.0	−120.0	−125.8	−126.4
C_1–C_2–C_3–C_5	−161.8	−160.6	−164.2	−160.6	−169.9	−159.2	−158.8	−156.6	−164.8	−158.5	−175.9	−158.3

C_1–C_2–C_3–H_8	−42.0	−44.7	−45.1	−44.8	−54.7	−45.2			−49.2	−44.6		
C_1–C_2–C_3–H_9	84.5	84.7	81.6	84.7			91.6	90.9			71.1	89.3
C_1–C_2–C_3–C_{14}					72.7	83.0	−36.0	−36.5	79.0	83.8	−57.4	−39.5
C_2–C_3–C_{14}–H_{15}					50.5	47.8	−51.8	−47.8	49.4	47.5	−48.5	−40.7
C_2–C_3–C_{14}–H_{16}					−69.4	−72.4	−172.0	−167.8	−70.6	−72.7	−168.1	−160.6
C_2–C_3–C_{14}–H_{17}					170.6	168.1	68.2	72.5	169.3	162.8	71.9	80.1
C_1–C_2–C_4–C_5	161.8	160.6	164.3	160.6	169.8	159.2	158.2	156.6	164.9	158.6	175.9	158.5
C_1–C_2–C_4–H_{10}	42.0	44.7	45.0	44.7	51.3	43.5	38.3	40.9	46.0	42.8	58.0	42.6
C_1–C_2–C_4–H_{11}	−84.5	−84.7	−81.6	−84.7	−74.8	−86.1	−88.4	−88.9	−80.5	−86.7	−68.2	−86.9
C_2–C_3–C_5–H_{12}	−132.0	−131.4	−130.5	−131.3	−125.8	−132.4	−134.8	−134.5	−129.6	−132.6	−121.9	−133.6
C_2–C_3–C_5–H_{13}	101.6	97.4	103.4	97.5	108.3	96.6	98.9	94.1	104.5	96.3	112.5	95.1
C_2–C_3–C_5–C_4	−12.3	−16.1	−10.9	−16.0	−7.1	−16.8	−14.4	−19.1	−10.2	−17.1	−3.4	−18.1

Table V. ^{13}C Chemical Shifts in Cycloadducts 20–23

	20	21	22	23
CH_{3a}	12.93	12.89	12.87	12.84
CH_{3b}	16.45	18.89	16.61	18.07
CH(CN)	23.70	25.34	24.59	25.76
CH_2	33.37	32.85	31.88	32.05
$CH(CH_3)$	39.39	44.17	40.36	45.04
$=CH(CH_3)$	118.40	118.75	117.03	116.10
=C	*a*	137.27	*a*	138.50

[a] Not observed.

the basis of the relative magnitudes of the long-range, allylic and homoallylic coupling constants. The results of NOE experiments have, however, allowed for the assignment of the stereochemistry. Irradiation of H_5 results in an increase in the intensity of the H_1 resonance in **22** of 3.4% and only a 0.5% increase in the intensity of H_1 in **20** and an increase in the intensity of the H_3 and H_4 resonances in **20** of 8.6% with no observable increase in the intensity of H_3 and H_4 in **22**. These data indicate that the stereochemistry about the exocyclic double bonds is that shown in structures **20** and **22**.

The ^{13}C NMR spectra of **20–23** have been recorded, and the ^{13}C chemical shifts are given in Table V. There is no discernable trend in the ^{13}C chemical shifts as a function of the stereochemistry about the exocyclic double bond as might have been anticipated. It is interesting to note that the ^{13}C chemical shifts of CH_{3b} and C_2 appear at slightly lower field in the cis isomers compared to that in the trans isomers.

In the cycloaddition reaction of 13DMA with ACN, four stereoisomeric diradical intermediates are formed, which are represented as **18a** and **18b** and **19a** and **19b**. **18a** and **18b** are related as enantiomers while **19a** and **19b** are related as diastereomers, each of which exists as a pair of enantiomers. Intermediates **18** and **19** are formed by the approach of the ACN as illustrated in **32** and **33**. The

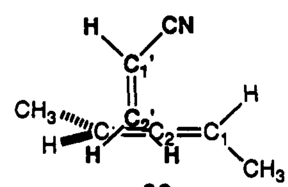

32

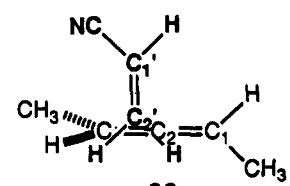

33

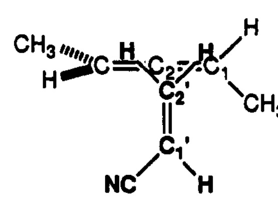

34

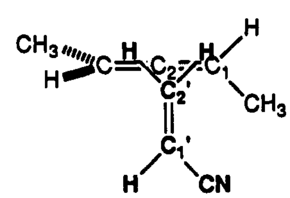

35

alternative approaches shown in **34** and **35** would ultimately result in the formation of cycloadducts possessing the *S* configuration at C_2 of the cycloadducts. We have investigated the lowest energy pathways for the approach of (*R*)-13DMA to the ACN in going to the activated complexes using the molecular mechanics approach and the molecular fitting and docking procedures incorporated in the CHEM-X program.[17] The structures of the (*R*)-13DMA and ACN were first individually optimized and were then docked such that the axis of the 2p AO on the central atom of 13DMA was aligned with the axis of the 2p AO of C_2 of the ACN with a separation distance of 2 Å. The MM2 energy surface was then computed as a function of the

(17) CHEM-X, developed and distributed by Chemical Design Ltd., Oxford.

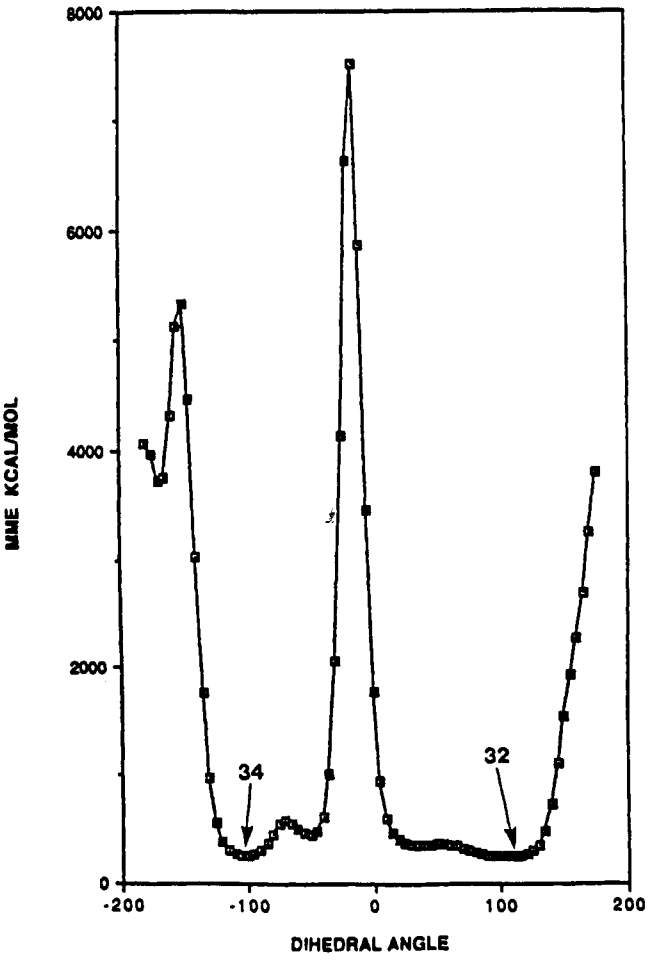

Figure 1. Plot of MM total energy versus C_1–C_2–C_2–C_1, dihedral angle for **32** (**34**).

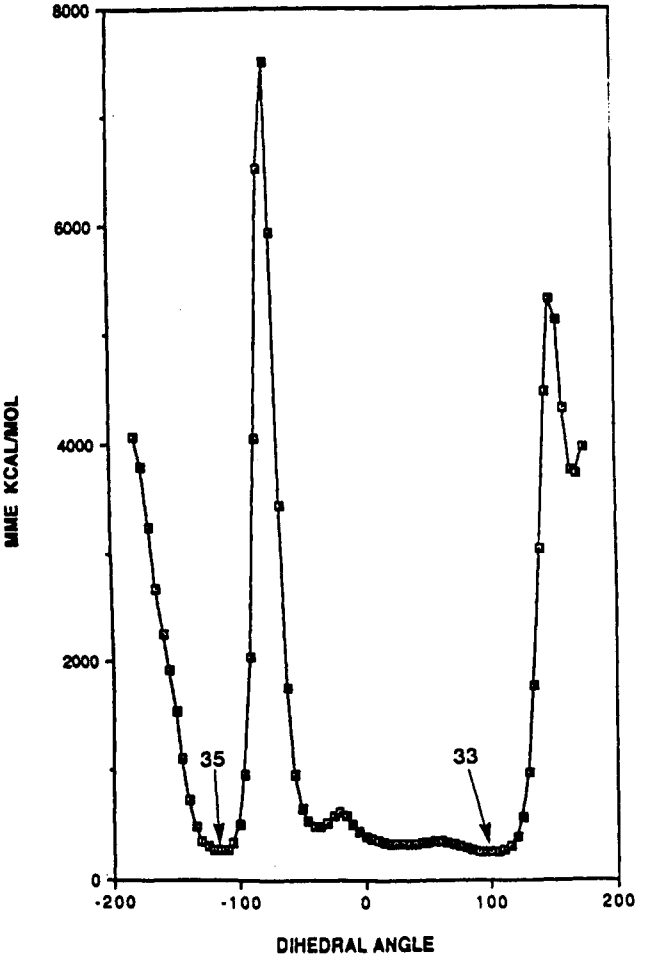

Figure 2. Plot of MM total energy versus C_2–C_2–C_2–C_1, dihedral angle for **33** (**35**).

C_1–C_2–C_2–C_1, dihedral angle for the two approaches to the ACN. (In **32**–**35**, the ACN, which is in front of the 13DMA, is indicated in bold-faced structures.) Figure 1 shows the energy profile for the orientation of the ACN as shown in **32** and **34**, while Figure 2 shows the energy profile for the orientation of the ACN as shown in **33** and **35**. The overall energy surface for the orientation of the ACN as shown in **32** and **34** is lower in energy than that for the orientation of the ACN as shown in **33** and **35**, with **32** and **33** representing the lowest energy approaches in the two orientations of the ACN. Approaches **32** and **33** to the activated complexes are the two approaches that lead to the configurations of the chiral intermediates first suggested by Baldwin and Roy,[6] which undergo ring closure to produce the *R* configuration in the cycloadducts.

An analysis of the possible modes of ring closure of **18** and **19** leads to a very reasonable interpretation of the product distribution observed in the cycloaddition reaction of 13DMA with ACN. Ring closure of intermediate **18a** to the left end of the allyl radical produces the *Z*,cis cycloadduct **21**, while ring closure to the right end produces the *Z*,trans cycloadduct **20**. Similarly, ring closure of **18b** produces either **20** or **21**. Of the two modes of ring closure of **18a** and **18b**, the ring closure to the trans cycloadducts should be favored because of less steric congestion in the transition states for ring closure. Ring closure of **19a** to the left end of the allyl radical produces the *E*,cis cycloadduct **23**, while ring closure to the right end produces the *Z*,cis cycloadduct **21**. The transition states for these two modes of ring closure should suffer roughly equivalent extents of steric congestion and should produce comparable quantities of **23** and **21**. Ring closure of **19b** to the left end of the allyl radical produces the *E*,trans cycloadduct **22**, while ring closure to the right end of the allyl radical produces the *Z*,trans cycloadduct **20**, again in comparable amounts. Overall, in view of the fact that **18a** and **19a** are predicted to be formed in preference to **18b** and **19b**, the cis isomers **21** and **23** are expected to be formed in preference to the trans isomers **20** and **22**. This is what is observed, but the preferences are slight.

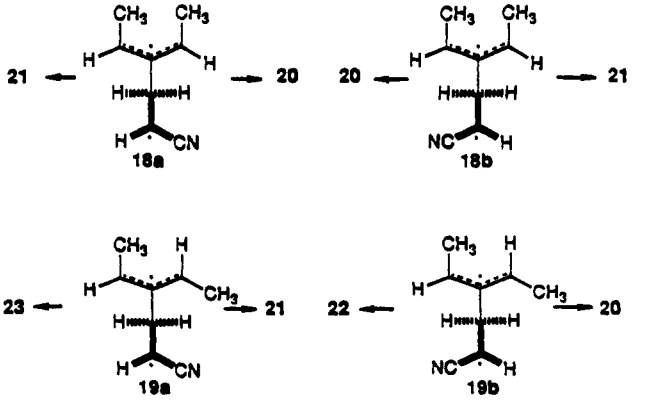

The *E*,Z product distribution of 58% **22** plus **23** and 42% **20** plus **21** suggests that diradical intermediates having the anti,syn stereochemistry about the allyl radical are formed in preference to the diradical intermediates having the anti,anti stereochemistry. This is in contrast with that observed in the cycloaddition of 13DMA with 1122 in which the anti,anti diradical intermediate is preferentially formed. One must inquire as to whether there has been a misassignment of the stereochemistry

Table VI. Chemical Shifts and Coupling Constants for 38–41

	38	39	40	41
	Chemical Shifts (δ)			
CH_{3a}	1.13	1.30	1.03	1.17
CH_{3b}	1.53	1.57	1.52	1.51
H_1	3.38	3.27	3.29	3.13
H_2	3.22	2.63	3.22	2.61
H_3	2.62	2.775	2.68	2.785
H_4	3.08	2.780	3.01	2.790
H_5	5.17	5.17	5.18	5.18
	Coupling Constants (Hz)			
H_1–H_2	6.69	8.27	9.37	7.84
H_2–H_4	8.48	8.27	8.52	7.84
H_2–H_3	7.77	6.56	5.75	9.08
H_1–H_5	1.92	2.55	1.84	2.37
H_3–H_5	1.74	1.98	2.69	2.49
H_4–H_5	2.74	1.98	2.86	2.49
H_1–H_3	1.76		~0.4	1.43
H_1–H_4	2.74		2.86	1.91
H_1–CH_{3a}	6.69	6.80	6.41	6.80
H_1–CH_{3b}	2.10	1.71	1.73	2.25
H_3–CH_{3b}	2.56	2.04	1.73	1.68
H_4–CH_{3b}	1.76	2.04	1.73	1.68
H_5–CH_{3b}	6.60	6.92	6.69	6.68

about the exocyclic double bond in the cycloadducts. Preliminary results derived from the cycloaddition of enantioenriched 13DMA with ACN suggest that the stereochemical assignments are in all probability correct. Cycloadducts derived from **18**, which contains a local vertical plane of symmetry in the allyl radical portion of the intermediate, should possess lower ee's than the cycloadducts derived from **19**, which does not possess a local vertical plane of symmetry in the allyl radical portion of the intermediate. The results of these preliminary experiments show that the cycloadducts assigned structures **20** and **21** possess very low ee's (relative to that of the starting 13DMA), while those assigned structures **22** and **23** possess moderately high ee's.[18] The possible reason(s) for the preferential formation of diradical intermediate **19** will be discussed in the concluding section of this paper.

Cycloaddition of 13DMA with Methyl Acrylate. The cycloaddition of 13DMA with MAC quantitatively produces the four cycloadducts **38–41** that could be partially separated by preparative GLC into pure fractions of **41** and **38** and mixtures rich in **39** and in **40** (the relative

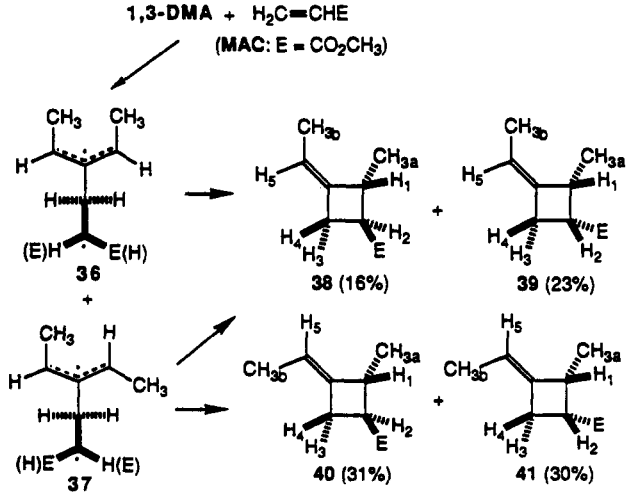

yields derived by integration of the NMR spectrum of the crude reaction mixture are given in parentheses under the structures). The NMR spectra of the mixtures rich in **39** and **40**, nonetheless, were sufficiently well-resolved that structural assignments could be made by comparison with the NMR spectral properties of the cycloadducts derived from 13DMA and ACN. The ^1H chemical shifts and coupling constants derived by extensive double resonance studies are given in Table VI.

As in the case of the cycloadduct derived from the cycloaddition of 13DMA with ACN, two of the cycloadducts, **39** and **41**, possess considerably higher field chemical shifts for H_2 typical of pseudoaxially oriented hydrogens as shown in conformations **25b** and **27b** (Scheme I, X = CO_2CH_3) of the cis cycloadducts **39** and **41**. The trend in the vicinal coupling constants between H_1, H_3, and H_4 with H_2 in **23** and **41** are similar in magnitude; however, the relative magnitudes of these coupling constants in **21** and **39** are reversed. The chemical shifts of H_3 and H_4 in **39** and **41** are very similar, whereas in **21** and **23** they were distinctly different. In the cycloadducts **39** and **41** it would appear that the two conformations of the two cycloadducts are comparably populated or that the long-range shielding effects of the ester function have a significant effect on the relative chemical shifts of H_3 and H_4. The stereochemistry about the exocyclic double bonds in **39** and **41** has been assigned as shown on the basis of the lower field chemical shifts of CH_{3a}, CH_{3b}, and H_1 in the *Z* isomer **39** relative to those in the *E* isomer **41**.

The chemical shifts of H_2 in the cycloadducts **38** and **40** appear at lower field than in **39** and **41**, indicating that **39** and **41** possess the same ring stereochemistry as in **20** and **22**. The inequality of the vicinal coupling constants between H_1 and H_4 with H_2 suggests that these cycloadducts exist in distorted conformations in which the H_1–H_2 and H_4–H_2 dihedral angles are not similar on a time-averaged basis. The stereochemistry about the exocyclic double bonds in **38** and **40** has been assigned as shown on the basis of the lower field chemical shifts of CH_{3a}, CH_{3b}, and H_1 in the *Z* isomer **38** compared to the *E* isomer **40**. A comparison of the relative yields of **38–41** with those of **20–23** show a similar trend as would be expected.

The predominant formation of **40** plus **41** over **38** plus **39** indicates that diradical intermediate **37** is formed in preference to **36**; again comparable to the preferred formation of **19** over **18** in the cycloaddition reaction of 13DMA with ACN. The ring closure of the diradical intermediates can be described as with **18** and **19**, and needs not be repeated.

Cycloaddition of 13DMA with *N*-Phenylmaleimide. The reaction of 13DMA with NPMI quantitatively produces a mixture of the four cycloadducts **44–47** that are cleanly separated by HPLC. The yields of the cycloadducts, based on the integration of the NMR spectrum of the original reaction mixture, are given in parentheses.

The stereochemistry of the ring substitution has been assigned on the basis of the relative magnitudes of the H_1–H_4 coupling constants (see Table VII). Molecular models indicate that the [3.2.0] bicyclic framework of the cycloadducts is quite rigid, with the four-membered ring being essentially planar. The coupling constants between cis-related hydrogens (dihedral angles of 0°) are thus expected to be significantly larger than between the trans-related hydrogens (dihedral angles of 120°). In all of the cycloadducts, the coupling constants between the cis-related hydrogens H_2 and H_3 fall in the range of 6.16–6.52 Hz. In cycloadducts **44** and **46**, the coupling constants between H_1 and H_2 are significantly smaller, being 3.21 and 3.78 Hz, respectively, indicating a trans relationship. In **45**, the H_1–H_2 coupling constant is considerably larger (9.98 Hz), indicating a cis relationship. The H_1–H_2 coupling

(18) Pasto, D. J.; Sugi, K. D. *J. Org. Chem.*, following paper in this issue.

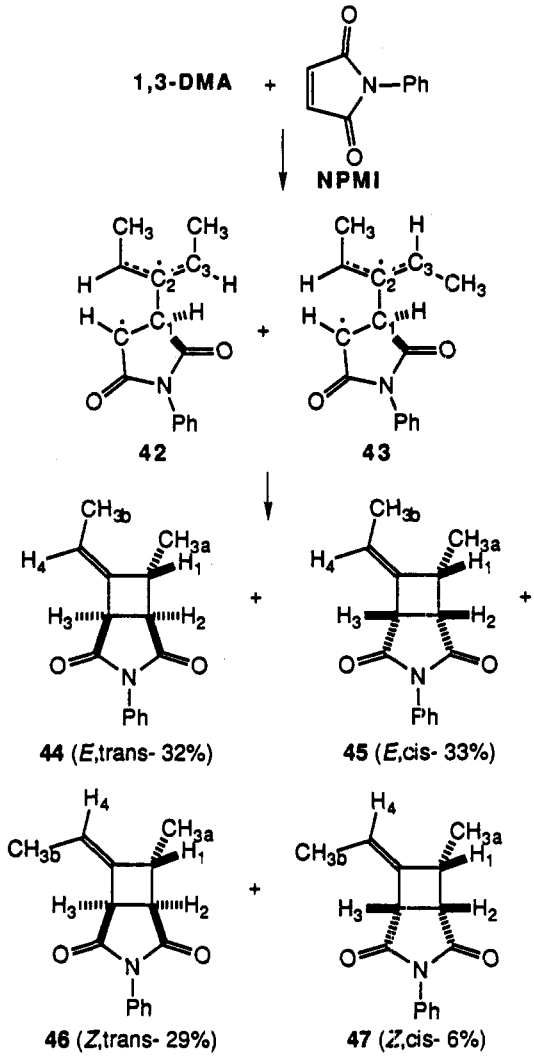

constant in **47** could not be determined because of the near identity in chemical shifts of H_1 and H_2. As two cycloadducts have been assigned the trans stereochemistry and only one the cis stereochemistry, **47** is assigned the cis stereochemistry by default.

The stereochemistry about the exocyclic double bonds in the cycloadducts has been assigned on the basis of the relative chemical shifts of CH_{3a}, CH_{3b}, and H_4. (It should be noted that the *E* and *Z* stereochemical designations for **44–47** appear to be reversed compared to the cycloadducts derived from 13DMA with ACN and MAC; however, this reversal is due to the change in the priorities of the groups attached to C_2 and C_4 of the methylenecyclobutane ring.) It has been previously noted that in the cycloadducts derived from the cycloaddition reactions of monoalkyl-substituted allenes with NPMI that when the allylic protons of groups attached to the exocyclic double bond are syn to the carbonyl group they appear at lower field than when anti.[2] On the basis of these criteria, the cycloadducts **46** and **47** with the lower field CH_{3b} resonances and higher field H_4 resonances are assigned the *Z* stereochemistry, while **44** and **45** with the higher field CH_{3b} resonances and lower field H_4 resonances are assigned the *E* stereochemistry. In the trans cycloadducts **44** and **46** the CH_{3a} resonance of the *E* isomer **44** appears at lower field than in the *Z* isomer **46**, while in the cis cycloadducts **45** and **47** the CH_{3a} resonance of the *E* isomer **45** appears at lower field than in the *Z* isomer **47**. All of the chemical shift correlations are consistent with the assigned stereochemistry about the exocyclic double bonds in the cycloadducts. It should be noted, however, that there is no consistent

Table VII. ^1H Chemical Shifts and Coupling Constants in 44–47

	44	45	46	47
	Chemical Shifts (δ)			
CH_{3a}	1.47	1.33	1.40	1.22
CH_{3b}	1.62	1.65	1.78	1.79
H_1	3.32	3.63	3.21	3.52
H_2	3.01	3.53	3.04	3.52
H_3	3.96	3.86	4.11	4.06
H_4	5.72	5.74	5.56	5.57
ArH	7.2–7.4	7.2–7.4	7.2–7.4	7.2–7.4
	Coupling Constants (Hz)			
H_1–H_2	3.21	9.98	3.78	[a]
H_2–H_3	6.51	6.36	6.52	6.16
H_1–H_4	2.25	2.59	2.05	1.96
H_3–H_4	2.25	2.19	2.62	2.65
H_1–CH_{3a}	7.10	7.21	7.01	6.86
H_1–CH_{3b}	1.38	1.89	2.28	2.28
H_3–CH_{3b}	2.01	1.94	1.63	1.57
H_4–CH_{3b}	7.00	7.05	6.93	6.93

[a] Could not be observed due to the essentially identical chemical shifts of H_1 and H_2.

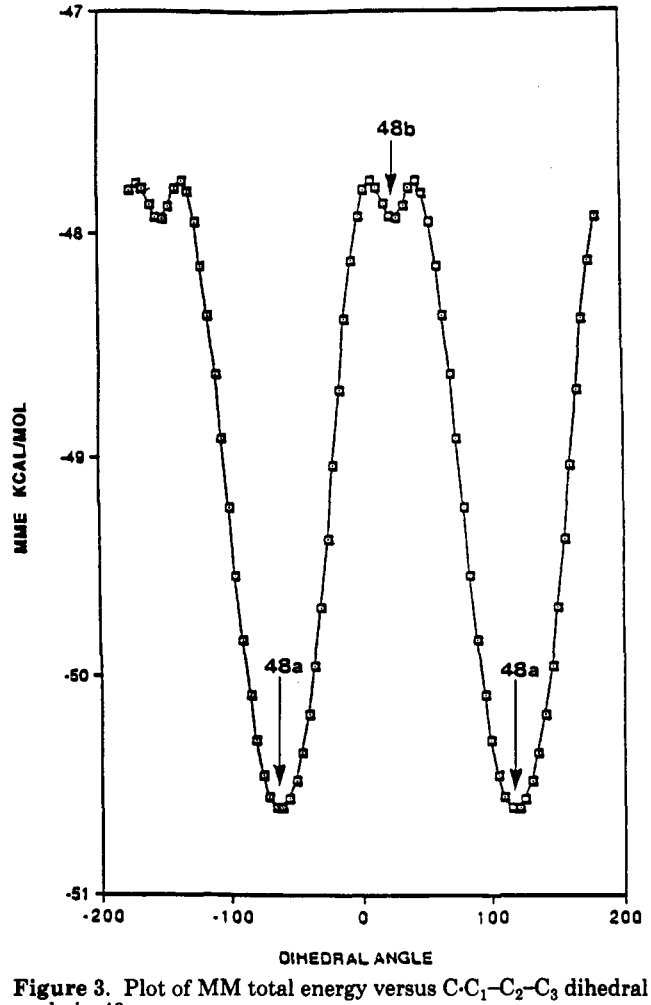

Figure 3. Plot of MM total energy versus C·C_1–C_2–C_3 dihedral angle in **48**.

correlation between the relative magnitudes of the long-range, allylic and homoallylic coupling constants with the assigned stereochemistry about the exocyclic double bonds in **44–47**.

In an attempt to analyze which cycloadduct, or cycloadducts, can be possibly formed by ring closure of the two diradical intermediates **42** or **43**, molecular mechanics calculations have been carried out using the CHEM-X program on **48** and **49** (R = R′ = CH_3) as models for **42** and **43**. (It must be pointed out that for convenience in visu-

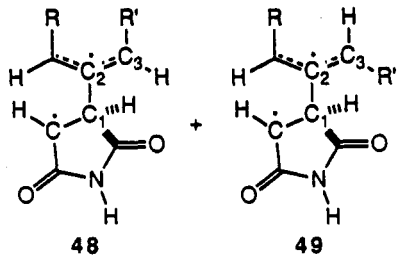

48 49

alizing the structures of the conformations of the diradical intermediates and their mode of formation and ring closure of the diradical intermediates **42** and **43** and **48** and **49**, the diradical intermediates shown have been formed by attack of (*R*)-13DMA on the *si* face of one of the vinyl carbon atoms of the NPMI. On ring closure, this will produce products having the *S* configuration at the methyl-bearing ring carbon, which is opposite to that observed by Baldwin and Roy[6] in the cycloaddition of 13DMA with ACN and consistent with the results of molecular mechanics calculations described previously.) The conformational energy surface of **48** has been calculated for a 360° rotation about the C–C_1–C_2–C_3 dihedral angle. The results of these calculations are shown in Figure 3. The two minimum ennergy conformations correspond to **48a** and its enantiomeric structure. The least motion ring

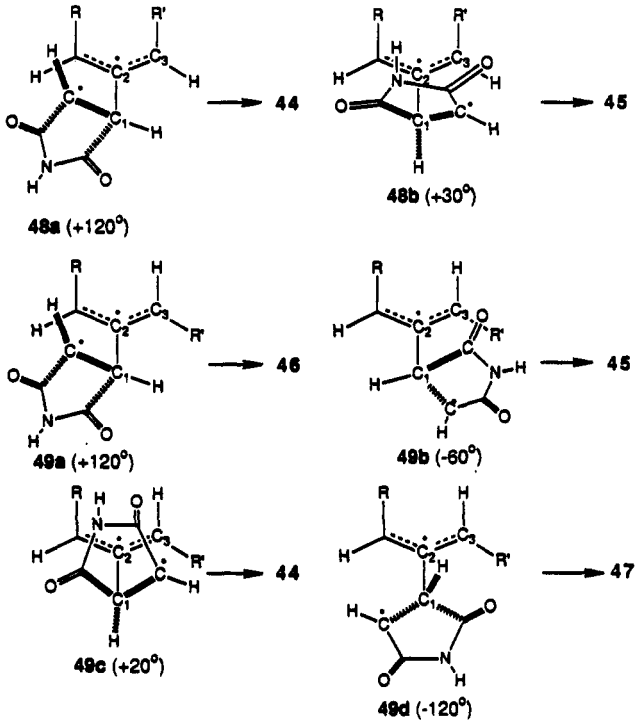

closure of **48a** and its enantiomer to the left end of the allyl radical produces the *E*,trans cycloadduct **44**. In order to form the *E*,cis cycloadduct **45**, the intermediate diradical must assume the conformation shown in **48b**. **48b** represents a high energy conformation on the energy surface of **48**, dihedral angle in the region of 0–60°, and is therefore not expected to contribute to the formation of **45**.

The optimized conformational energy surface of **49** is shown in Figure 4. The two minimum energy conformations shown in Figure 4 possess structures **49a** with a dihedral angle of ~+120° and **49b** with a dihedral angle of ~–60°. The least motion ring closure of **49a** produces the *Z*,trans cycloadduct **46**, while the least motion ring closure of **49b** produces the *E*,cis cycloadduct **45**, which was predicted not to be produced by the ring closure of **48**. The formation of the *E*,trans cycloadduct **44**, which is predicted to be favored in the ring closure of **48a**, re-

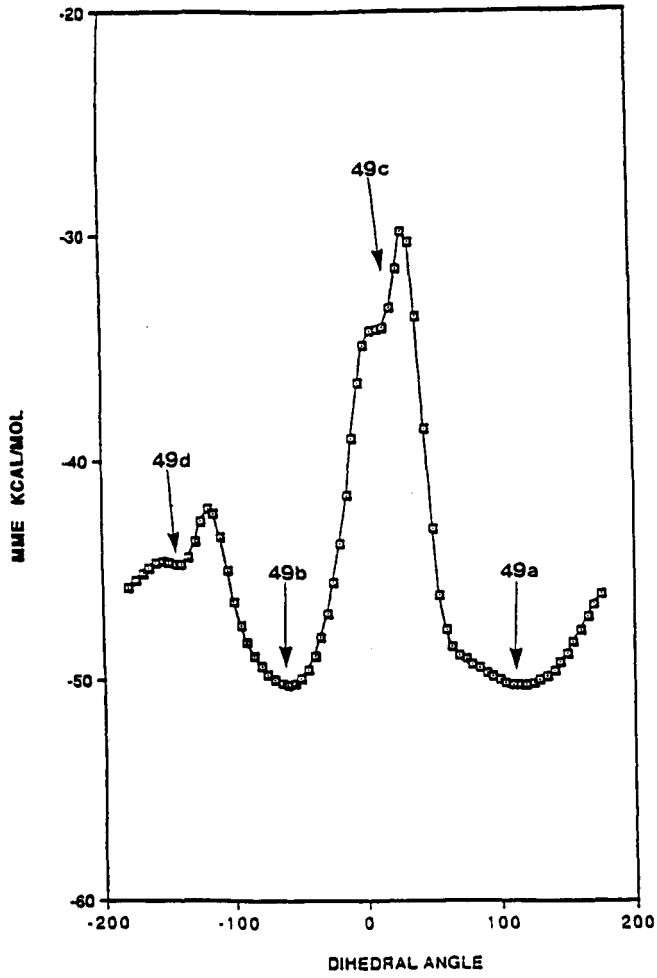

Figure 4. Plot of MM total energy versus C·C_1–C_2–C_3 dihedral angle in **49**.

quires the conformation shown in **49c**, which is near energy maximum conformation with a dihedral angle of ~+10°. The formation of the *Z*,cis cycloadduct **47**, which cannot be formed from **48**, requires adopting the higher energy conformation **49d** with a dihedral angle of ~–140°, leading to the prediction that the formation of **47** should not be very favorable. This is fully consistent with the observed product distribution.

Thus, the overall conclusions that one must draw from the results of the cycloaddition of 13DMA with NPMI are the following: (1) Only **44** is formed from **42**. (2) Cycloadducts **45**–**47** are formed predominately from **43**, with **47** expected to be formed in very low yield. Considering the relative yields of the four cycloadducts, it must then be concluded that the formation of **43** is significantly favored over the formation of **42** (68:32). This is in significant contrast to the results of the cycloaddition reactions of monoalkyl-substituted allenes with NPMI in which it was previously concluded that predominant product formation occurred via the anti alkyl-substituted diradical intermediates.[2] This difference will be addressed in the final section of this paper.

The final point to consider is what conformation of the reactants is favored in the approach to the activated complex(es) leading to diradical intermediate formation. The structure of the NPMI was optimized by molecular mechanics calculations using the CHEM-X program and was docked to the 13DMA with a separation distance of 2 Å as described previously for the calculations on 13DMA with ACN. The conformational energy surface was calculated for a 360° rotation about the C_1–C_2–C_3–C_4 bond. The

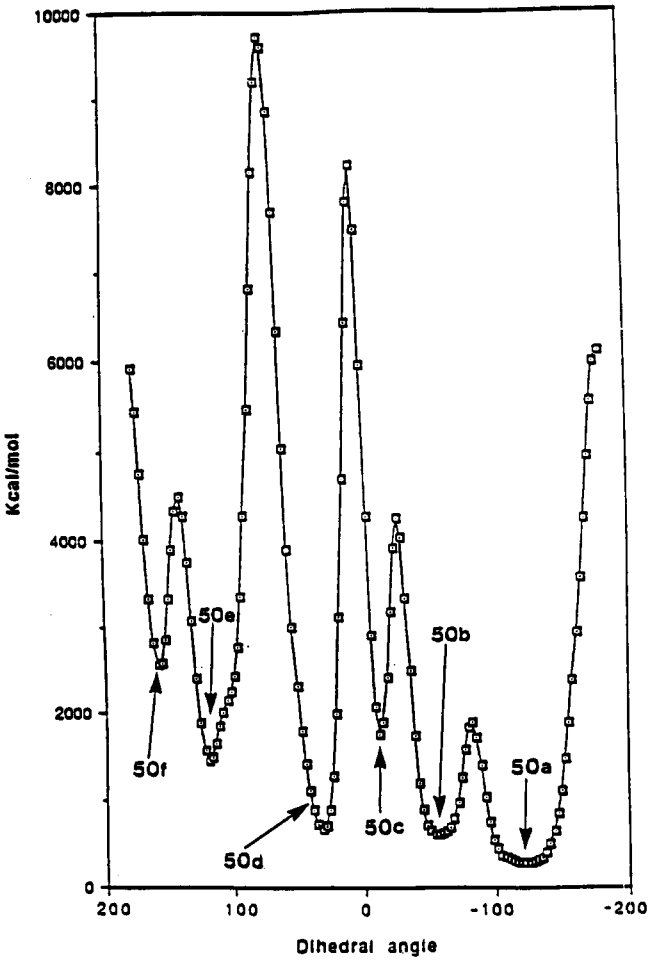

Figure 5. Plot of MM total energy versus C_1–C_2–C_3–C_4 dihedral angle in **50**.

conformational energy surface is very complex, showing six minima (see Figure 5). The lowest energy conformation is that shown as **50a**, which is considerably lower in

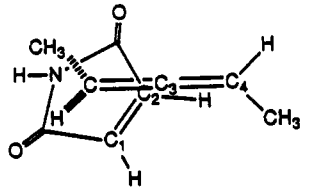

50a (-122°, 281.7)

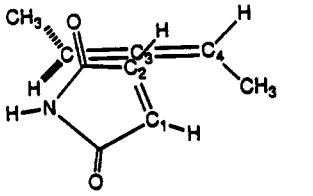

50b (-57°, 430.9)

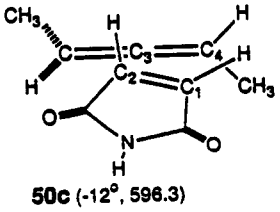

50c (-12°, 596.3)

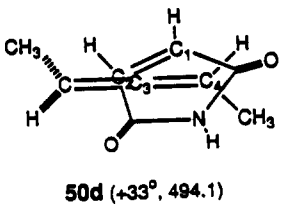

50d (+33°, 494.1)

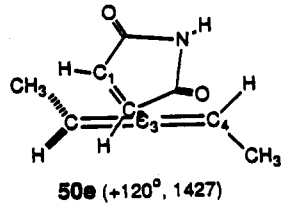

50e (+120°, 1427)

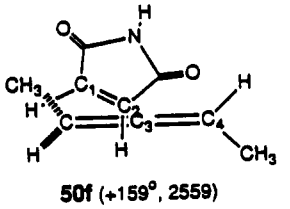

50f (+159°, 2559)

energy than the other conformations **50b–f**. (The numbers in parentheses are the C_1–C_2–C_3–C_4 dihedral angles and the MME energies (kcal mol^{-1}), the differences of which are essentially totally due to differences in long-range interactions.) On proceeding to **42** and **43**, conformation **50a** directly produces conformations corresponding to **48a** and **49a**, which are the lowest energy conformations of **48** and **49**! It is not obvious, however, which of the minimum energy conformations shown give rise to **49b**, which would appear to be the most logical precursor of diradical intermediate for **45**.

Cycloaddition of 13DMA with Diethyl Fumarate and Diethyl Maleate. The reaction of 13DMA with DEF produces a mixture of the two minor cycloadducts **54** and **56** and the two major cycloadducts **53** and **55**, which could be separated with great difficulty into fractions of **54–56** and a mixture of **53** and **55** by preparative GLC. The relative yields are shown in the parentheses below the structures along with the stereochemical designations for the exocyclic double bonds and ring substitution.

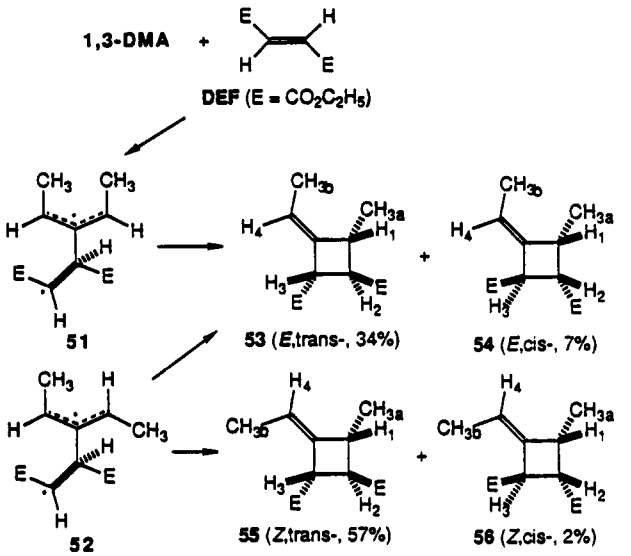

The stereochemistry of ring substitution at C_2 and C_3 has been assigned on the basis of comparisons of the relative chemical shifts of CH_{3a} and H_1 with those observed in the cycloadducts derived with MAC and the relative magnitudes of the vicinal coupling constants between H_1 and H_2. In the *trans*-MAC cycloadducts, CH_{3a} appears at higher field than in the cis isomers, while H_1 appears at lower field than in the cis isomers. Similar trends are observed in the NMR spectra of the DEF cycloadducts, indicating that **53** and **55** possess the trans stereochemistry, while **54** and **56** possess the cis stereochemistry. The assignment of trans stereochemistry to **53** and **55** is also consistent with the large vicinal coupling constants between H_1 and H_2 (9.90 and 10.57 Hz, see Table VIII) in conformations where H_1 and H_2 are both pseudoaxial. In **54**, the vicinal coupling constant between H_1 and H_2 is much smaller (3.30 Hz), which is consistent with a pseudoequatorial–pseudoaxial relationship. These stereochemical assignments have been made based on the assumption that the long-range shielding effects of the two ester functions on H_1 are negligible and that the presence of all of the functionality on the four-membered ring does not result in distortions of the ring resulting in changes in the relative magnitudes of the vicinal coupling constants between H_1 and H_2. Insufficient quantities of **56** were obtained pure enough to derive a sufficiently well-resolved NMR spectrum to determine all of the coupling constants; however, by default the stereochemical relationship between the methyl and ester functions must be cis.

Table VIII. ^{1}H Chemical Shifts and Coupling Constants for 53–56

	53	54	55	56
	Chemical Shifts (δ)			
CH_{3a}	1.12	1.33	1.04	1.26
CH_{3b}	1.54	1.58	1.61	1.56
H_1	3.35	3.16	3.42	3.01
H_2	3.56	3.69	3.55	3.61
H_3	4.15	3.83	4.21	3.94
H_4	5.46	5.47	5.32	5.32
CH_2[a]	4.15	4.16	4.14	4.14
CH_2	4.15[b]	4.14, 4.17	4.11, 4.12	4.17, 4.18
CH_3[c]	1.25	1.26	1.25	1.27
CH_3	1.25	1.24	1.25	1.24
	Coupling Constants[d] (Hz)			
H_1–H_2	9.90	3.30	10.57	[e]
H_2–H_3	7.90	7.38	5.28	[e]
H_1–H_4	2.40	2.6	2.74	[e]
H_3–H_4	2.66	2.6	2.50	[e]
H_1–CH_{3a}	7.34	6.86	7.00	7.04
H_4–CH_{3b}	6.84	7.06	6.91	7.01
H_1–CH_{3b}	1.39	2.34	2.16	[e]
H_3–CH_{3b}	2.55	1.94	1.79	[e]
CH_2–CH_3	7.06	7.08	7.12	7.10
CH_2–CH_3	7.06	7.12	7.12	7.10

[a] The hydrogen atoms of the methylene group of one of the esters did not show diastereotopic character. [b] Diastereotopicity could not be detected. [c] The relationships between the methyl and methylene groups could not be established on the basis of the coupling constants. [d] Cross-ring coupling constants were not observable. [e] Could not be determined.

The assignment of the stereochemistry about the exocyclic double bonds in the trans cycloadducts **53** and **55** is based on the lower field chemical shift of CH_{3b} in **55** and the lower field chemical shifts of H_4 and CH_{3a} in **53** as observed in the cycloadducts derived with the other dienophiles as described previously. Similarly, the assignment of the stereochemistry about the double bonds in the cis cycloadducts **54** and **56** is based on the observed lower field chemical shifts of H_4 and CH_{3a} in **54** relative to **56**. This assignment of the stereochemistry about the exocyclic double bonds in **53** and **55** is supported by the observed long-range, allylic and homoallylic coupling constants. The long-range allylic coupling constant between H_3 and H_4 in **53** (2.66 Hz) is larger than that between H_3 and H_4 in **55** (2.50 Hz), and the allylic coupling constant between H_1 and H_4 in **55** (2.74 Hz) is larger than that in **53** (2.40 Hz), while the homoallylic coupling constant between H_1 and CH_{3b} in **55** (2.16 Hz) is larger than that in **53** (1.39 Hz), and the homoallylic coupling constant between H_3 and CH_{3b} in **53** (2.55 Hz) is larger than that in **55** (1.79 Hz).

The reaction of 13DMA with DEM proceeds rather slowly compared to the reaction of 13DMA with DEF and produces a mixture of only the trans diester cycloadducts **53–56** as indicated by GLC and NMR analysis. The ratio of the cycloadducts derived in the reaction with DEM is, within experimental error, identical with that derived with DEF. In addition, extensive isomerization of DEM to DEF is observed, which has been shown previously not to occur under the reaction conditions in the absence of an allene.[1] These results indicate that the diradical intermediates **57** and **58** initially formed with DEM, in which the two ester functions are initially synperiplanar, undergo internal rotation to form the lower energy conformation diradical intermediates **51** and **52**, which are directly formed in the reaction of 13DMA with DEF in which the two ester functions are probably nearly antiperiplanar. (The structures drawn for **51** and **52** and **57** and **58** are intended to illustrate only the conformational relationships between the two ester *E* groups and are not intended to illustrate a preferred conformation about the newly formed C–C bond in the intermediates.)

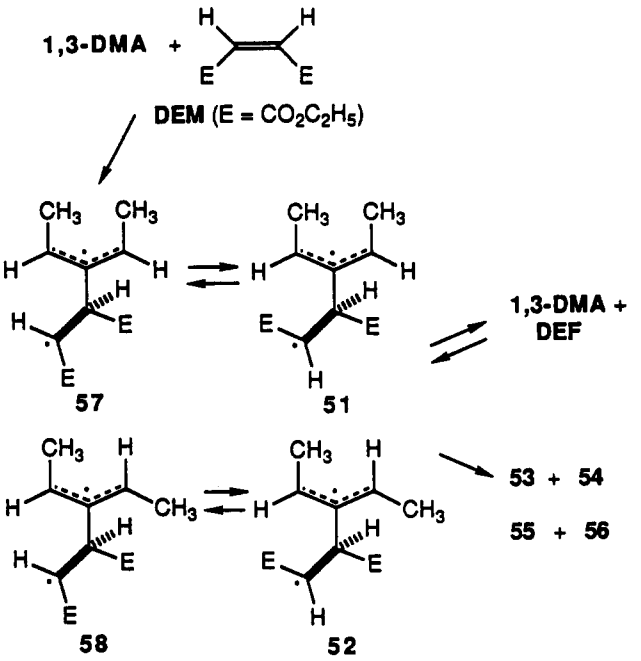

In the cycloaddition reactions of 13DMA with DEF with DEM, the apparent reversibility of diradical intermediate formation precludes a definitive discussion of the lowest energy, irreversible pathways for diradical intermediate formation that would ultimately dictate the product distribution. It must be noted, however, that the cycloadducts having the *Z* stereochemistry about the exocyclic double bond dominate, suggesting that diradical intermediate **52** is the predominant diradical intermediate leading to cycloadduct formation in the reaction of 13DMA with DEF.

Summary

The *E,Z* product distribution observed in the cycloaddition reaction of 13DMA with 1122 is consistent with the predominant formation of the anti,anti diradical intermediate **14**. These results are also consistent with our earlier observations on the cycloaddition reactions of monoalkyl-substituted allenes with 1122, which have been interpreted in terms of the reactions proceeding via the predominant formation of the diradical intermediates **1**. However, the results obtained from the cycloaddition reactions of 13DMA with ACN, MAC, and NPMI suggest that the anti,syn diradical intermediates **19**, **37**, and **43** are formed in preference to the anti,anti diradical intermediates. The results derived from the cycloaddition reactions of 13DMA with DEF and DEM do not allow for any interpretation in terms of the preference for the formation of either the anti,anti or anti,syn diradical intermediates.

What are the possible causes for this reversal in the stereochemical trend for the formation of the diradical intermediates? One reason could be the reversible formation of the diradical intermediates in the cycloaddition reactions with ACN, MAC, and NPMI, with the anti,syn diradical intermediates being thermodynamically favored. The second reason could be that the transition states for formation of the diradical intermediates occur at slightly different extents along the reaction coordinate. It is possible that the transition states for diradical intermediate formation with 1122 occur slightly earlier along the reaction coordinate in which the interaction between the alkyl group on the rotating end of the sbstituted allene with the approaching 1122 is more important than the steric re-

pulsion between the two methyl groups in the anti,anti diradical intermediate, while in the cycloaddition reaction of 13DMA with ACN, MAC, and NPMI the transition states occur later along the reaction coordinate in which the steric repulsion between the two methyl groups leading to the anti,anti diradical intermediates is greater than that between the methyl group and the approaching dienophile. The resolution between these two alternative can only be achieved by the results of a study of the cycloaddition reactions of an optically active allene with ACN, MAC, and NPMI, as well as other possible radicophiles. Such studies are currently in progress.

Experimental Section

General Procedures. Periodic monitoring of the following reaction mixtures by NMR spectroscopy shows that the ratios of the products do not change with time.

Cycloaddition of 1,3-Dimethylallene with 1,1-Dichloro-2,2-difluoroethene. To 140 mg (2.06 mmol) of 13DMA in an NMR tube was condensed 0.6 mL of 1122 at dry ice temperature. The contents of the tube were triply freeze–degassed, and the tube was sealed under reduced pressure. The tube was heated in a sand bath at 160 °C for 48 h, after which analysis by 300-MHz ^{1}H NMR indicated the complete disappearance of the 13DMA and the formation of the two cycloadducts **16** and **17** in a 66.6:33.4 ratio. There was no evidence for the formation of any polymeric material. The tube was chilled in ice–water and carefully cracked open. The 1122 was allowed to evaporate, and the cycloadducts were isolated by preparative GLC on a 12 ft × $^1/_4$ in. Carbowax 20M on Chromosorb P column. The 300-MHz ^{1}H NMR data of the two cycloadducts **16** and **17** are given in Table I, and the spectra are provided in the supplementary material. ^{19}F NMR (relative to external BF_3-etherate): **16** 54.0 (dqd, J = 197, 3.1, 3.1 Hz) and 56.4 (dm, J = 197 Hz); **17** 52.3 (dqd, J = 200, 3.1, 3.1 Hz) and 54.7 (dqd, J = 200, 2.2, 1.9 Hz). HRMS: calcd for $C_7H_8{}^{35}Cl_2F_2$ 199.9971, obsd **16**, 199.9970; **17**, 199.9970.

Cycloaddition of 13DMA with Acrylonitrile. In an NMR tube were placed 140 mg (2.06 mmol) of 13DMA, 645 mg (12.15 mmol) of ACN, 0.5 mL of toluene-d_8, and 10 mg of hydroquinone. The contents of the tube were triply freeze–degassed, and the tube was sealed under reduced pressure and then heated in a sand bath at 160 °C for 5 d, after which time analysis by NMR showed the complete disappearance of the 13DMA and the presence of the four cycloadducts **20–23** in a ratio of 18:24:25:33. There was no evidence for the formation of any polymeric material. The tube was opened, and the volatiles were removed on a vacuum line. The mixture of the cycloadducts was separated by preparative GLC on a 37 ft × $^1/_4$ in. Carbowax 20M on Chromosorb P column at 210 °C. The 300-MHz ^{1}H NMR data of the four cycloadducts **20–23**, derived by extensive double resonance experiments, are given in Table II, and the spectra are provided in the supplementary material. The ^{13}C chemical shifts are given in Table III. NOE experiments were carried out on **20–23**, the results of which are described in the text. HRMS: calcd for $C_8H_{11}N$ 121.0892, obsd **20**, 121.0890; **21**, 121.0890; **22**, 121.0890; **23**, 121.0890.

Cycloaddition of 13DMA with Methyl Acrylate. In an NMR tube were placed 140 mg (2.06 mmol) of 13DMA, 89 mg (1.03 mmol) of MAC, 0.6 mL of toluene-d_8, and 5 mg of hydroquinone. The contents of the tube were triply freeze–degassed, and the tube was sealed under reduced pressure and heated in a sand bath at 160 °C for 3 d, after which time analysis by NMR indicated the complete disappearance of the 13DMA and showed the presence of only the four cycloadducts **38–41** in a ratio of 16:23:31:30. There was no evidence for the formation of any polymeric material. The tube was opened and the volatiles were removed on a vacuum line. The mixture of the cycloadducts was separated by preparative GLC on a 39 ft × $^1/_4$ in. Carbowax 20M on Chromosorb P at 190 °C. The 300-MHz ^{1}H NMR spectral data for **38–41** are given in Table IV, and the spectra are provided in the supplementary material. MS: no parent ion in EIMS, m/e 155 in isobutane CIMS.

Cycloaddition of 13DMA with *N*-Phenylmaleimide. In an NMR tube were placed 140 mg (2.06 mmol) of 13DMA, 200 mg (1.16 mmol) of NPMI, and 0.6 mL of toluene-d_8. The contents of the tube were triply freeze–degassed, and the tube was sealed under reduced pressure. The tube was heated in a sand bath at 160 °C for 4 d, after which time NMR analysis indicated the complete disappearance of the NPMI and the presence of only the four cycloadducts **44–47** in a ratio of 32:33:29:6. There was no evidence for the formation of any polymeric material. The tube was opened, and the volatiles were removed on a vacuum line. The mixture of cycloadducts was separated by preparative HPLC on a 220 × 4.6 mm silica gel column using a 90:10 ratio of hexane–ethyl acetate as eluent, giving four well-resolved fractions. The 300-MHz ^{1}H NMR spectral data of the four cycloadducts are given in Table VII, and the spectra are provided in the supplementary material. HRMS: calcd for $C_{15}H_{15}NO_2$ 241.1103, obsd **44**, 241.1104; **45**, 241.1100; **46**, 241.1100; **47**, 241.1102.

Cycloaddition of 13DMA with Diethyl Fumarate. In an NMR tube were placed 80 μL of 13DMA and 450 μL of DEF.[19] The contents of the tube were triply freeze–degassed, and the tube was sealed under vacuum and then heated in a sand bath at 160 °C for 5 d, after which time analysis by NMR indicated the complete disappearance of the 13DMA and the formation on only the four cycloadducts **53–56** in a ratio of 34:7:57:2. There was no evidence of any oligomerization or polymerization products. The tube was opened, and the excess DEF was removed on a vacuum line. The mixture of the cycloadducts was partially separated by preparative GLC on a 12 ft × $^1/_4$ in. Carbowax 20M on Chromosorb P column, giving pure fractions of **53**, **54**, and **56** and a fraction containing a mixture of **53** and **55** rich in **55**. The 300-MHz ^{1}H NMR data for **53–56** are given in Table V, and the spectra are included in the supplementary material. HRMS: calcd for $C_{13}H_{20}O_4$ 240.1362, obsd **53**, 240.1364; **54**, 240.1364; **55**, 240.1364; **56**, 240.1364.

Cycloaddition of 13DMA with Diethyl Maleate. The cycloaddition of 13DMA with DEM was carried out as described for the reaction with DEF. Analysis of the crude reaction by NMR and GLC indicated the presence of only the trans diester cycloadducts **53–56** and DEF.

Acknowledgment. We acknowledge support of this research by the National Science Foundation (Grant No. CHE8709725) and the National Center for Supercomputing Applications at the University of Illinois for a grant of computer time.

Supplementary Material Available: 300-MHz ^{1}H NMR spectra of all cycloadducts (31 pages). Ordering information is given on any current masthead page.

(19) When this cycloaddition reaction was carried out in toluene-d_8 solution, extensive 1,3 sigmatropic rearrangement of 13DMA occurred to produce a mixture of (*E*)- and (*Z*)-1,3-pentadienes that then underwent cycloaddition with the DEF.